Taylor & Francis
Taylor & Francis Group

🔓 OPEN ACCESS

Assessment of an innovative seat belt with independent control of the shoulder and lap portions using THOR tests, the THUMS model, and PMHS tests

Bengt Pipkorn[a], Francisco J. López-Valdés[b], Oscar Juste-Lorente[b], Ricardo Insausti[c], Christer Lundgren[a], and Cecilia Sunnevång[a,d]

[a]Autoliv Research, Vårgårda, Sweden; [b]Impact Laboratory (I3A), University of Zaragoza, Zaragoza, Spain; [c]Human Neuroanatomy Laboratory, School of Medicine, University of Castilla-La Mancha, Albacete, Spain; [d]Department of Surgical and Perioperative Science, Umeå University, Umeå, Sweden

ABSTRACT

Objectives: The objective of this study was to determine the potential chest injury benefits and influence on occupant kinematics of a belt system with independent control of the shoulder and lap portions.

Methods: This article investigates the kinematics and dynamics of human surrogates in 35 km/h impacts with 2 different restraints: a pretensioning (PT), force-limiting (FL) seat belt, a reference belt system, and a concept design with a split buckle consisting (SB) of 2 separate shoulder and lap belt bands. The study combines mathematical simulations with the THOR dummy and THUMS human body model, and mechanical tests with the THOR dummy and 2 postmortem human surrogate (PMHS) tests of similar age (39 and 42 years) and anthropometry (62 kg, 181 cm vs. 60 kg, 171.5 cm). The test setup consisted of a rigid metallic frame representing a standard seating position of a right front passenger. The THOR dummy model predictions were compared to the mechanical THOR dummy test results. The THUMS-predicted number of fractured ribs were compared to the number of fractured ribs in the PMHS.

Results: THOR sled tests showed that the SB seat belt system decreased chest deflection significantly without increasing the forward displacement of the head. The THOR model and the THOR physical dummy predicted a 13- and 7-mm reduction in peak chest deflection, respectively. Peak diagonal belt force in the mechanical test with the reference belt was 5,582 N and the predicted force was 4,770 N. The THOR model also predicted lower belt forces with the SB system than observed in the tests (5,606 vs. 6,085 N). THUMS predicted somewhat increased head displacement for the SB system compared to the reference system. Peak diagonal force with the reference belt was 4,000 N and for the SB system it was 5,200 N. The PMHS test with the SB belt resulted in improved kinematics and a smaller number of rib fractures (2 vs. 5 fractures) compared to the reference belt.

Conclusion: Concepts for a belt system that can reduce the load on the chest of the occupant in a crash and thereby reduce the number of injured occupants, in particular the elderly, was proposed.

Introduction

The 3-point belt is a generally accepted and effective way to restrain vehicle occupants in a frontal impact. The overall life-saving effectiveness was estimated as 61% (Cummings et al. 2003). Nevertheless, performance can be improved. Pretensioned and force-limiting seat belts in combination with airbags was shown to significantly reduce thoracic loading and consequently thorax injuries for a driver (Kent et al. 2001; Walz 2004). In addition, inflatable belts have been introduced in several vehicle models across different manufacturers. Despite the fact that the intention with these system is to improve the performance in 3-point seat belt geometry, the implementation is limited due to the complexity of the system. A 4-point belt system in the form of a V was also suggested and evaluated (Rouhana et al. 2003). The V-shaped 4-point belt with pretensioner and force-limiting and inflatable belts were evaluated by means of

postmortem human surrogate (PMHS) tests. In frontal impacts the protective effect of the systems was confirmed (Rouhana et al. 2003). It was suggested that by engaging additional bony structures of the body such as the clavicle the load on the ribs can be reduced. An evaluation of a system with a separated diagonal and lap portion of the belt with the aim to add more load to the upper part of the body such as the clavicle was carried out using THOR, PMHS tests, and human body modeling. Reductions in chest deflections for the THOR dummy were obtained with a system with separated diagonal and lap portions of the belt relative to a state-of-the-art belt system used in the vehicles sold today (López-Valdés and Juste-Lorente 2015; Pipkorn et al. 2015). However, limited evaluation of the injuries sustained by the PMHS was published.

Injuries to the chest consists of rib fractures, sternum fractures, lung contusions, etc. Fractured ribs are not necessarily life threatening. However, elderly adults hospitalized after a car

---

CONTACT Bengt Pipkorn ✉ bengt.pipkorn@autoliv.com 🖅 Autoliv Research, Wallentinsv 22, 44783 Vårgårda, Sweden.
Color versions of one or more of the figures in the article can be found online at www.tandfonline.com/gcpi.
Associate Editor Matthew Maltese oversaw the review of this article.
🔗 Supplemental data for this article can be accessed on the publisher's website.

crash can die from only a few fractured ribs (Kent et al. 2001, 2008). As the aging population and requirements of mobility are increasing worldwide, rib fracture countermeasures for seniors are becoming increasingly important.

Life expectancy in Europe was increased by 8 years between 1960 and 2006 (Roser 2006), which means that the average age of car buyers in Europe also increased. It is also the fact that increased frailty and fragility are associated with aging. A review of Abbreviated injury Scale (AIS) 3+ injuries within the NASS-CDS found that as age increases from 15 to 75+ years old, the incidence of thoracic injuries increases and becomes the most frequent serious injury among car occupants older than 46 years old, accounting for more than 35% of all AIS3+ injuries in people aged 75 years and above (Scarboro 2014). Therefore, given the existing trend of a growing proportion of elderly road users, it is mandatory to recognize their physiological differences and to incorporate their peculiarities into the design of more effective restraints.

Previous studies have shown that THOR exhibits improved kinematic and thoracic biofidelity compared to the Hybrid III dummy (Parent et al. 2013; Shaw et al. 2009). In addition, the THOR (a THOR version similar to the Mod-Kit SD3 shoulder) was shown to be more sensitive to restraint variation and impact severity compared to the Hybrid III (Sunnevång et al. 2014). The THOR-M is proposed to replace the Hybrid III dummy for the full frontal impact in an update of the U.S. New Car Assessment Program (Department of Transportation 2015). With its improved biofidelity and sensitivity, the THOR can be an applicable tool for assessing thoracic injuries to the elderly population.

With the continuous improvement of finite element human body models, parametric analyses constitute an effective methodology to optimize the design of new restraint systems for reducing occupant injury risk. Therefore, to efficiently evaluate the potential injury-reducing benefits of restraint systems, a combination of human body modeling, anthropomorphic test device (ATD) modeling, ATD testing, and PMHS testing seems to be applicable. Thus, PMHS testing can confirm the potential benefit that these system can bring to car occupants (young and elderly) that were found by human body model and THOR evaluations. The goal of this article is to compare the potential thoracic injury-reducing benefit of an innovative seat belt system with independent shoulder and lap belts to a state-of-the-art seat belt as predicted by the different types of surrogates, THOR,

THUMS, and PMHS. In particular the potential injury-reducing benefits for the PMHS were evaluated.

Methods

The evaluation of the proposed seat belt system, split buckle (SB), was carried out by combining mathematical modeling with mechanical testing (López-Valdés and Juste-Lorente 2015; Pipkorn et al. 2015). The sled test fixture consisted of a rigid flat horisontal steel seat and steel wire seat back, allowing complete visual access to the occupant while preserving the basic geometry of a standard seating position of a passenger car. This test fixture was developed as a reasonable approximation to the passenger posture in the study of ATD biofidelity and in the development of thoracic injury criteria (López-Valdés et al. 2010; Shaw et al. 2009). In these tests, the knee bar previously used in the aforementioned references was removed from the fixture. The rigid seat was considered to be a worst-case scenario for the occupant due to the fact that no antisubmarining system was included. However, due to the fact that pelvis pretensioners were used, the risk of the occupant submarining in the tests was limited. In another study, a modification of the rigid seat structure to make it more similar to a vehicle seat was evaluated (Pipkorn et al. 2016).

The 50th percentile THOR finite element (FE) model (THOR-M version 0.6; Humanetics 2014) was used to evaluate the test environment (seat and seat belt) by matching predictions from the model to experimentally measured THOR test responses (Figure 1). The THOR ATD used in this study is the THOR-NT upgraded within the THORAX project (European 7th Framework Program) to improve biofidelity and injury assessment capabilities. This THORAX THOR (further denoted simply as THOR) is similar to the U.S. version THOR Mod Kit with SD3 shoulder. For both mechanical and mathematical THOR, the lumbar angle adjustment was set to mid-position, and peak resultant deflection was used to assess occupant thoracic injury risk. The injury risk curve (IRC) for peak resultant deflection presented by Saunders et al. (2015) was used to predict the injury risk to a 45-year-old occupant as well as a 65-year-old occupant. The IRC derived for the mechanical THOR was also used for the THOR FE in the same manner. The impact velocity ranged from 35 to 38 km/h and peak acceleration from 16 to 19 g for a duration of approximately 80 ms (Figures A1 and A2, see online supplement), based on the field analysis reported by Gabler et al. (2005) describing the total struck-vehicle delta-V of tow-away far-side impact collisions (NASS-CDS 1993–2002). A similar crash pulse had been used in Forman et al. (2013) in PMHS sled tests in far-side oblique impacts. The crash pulse from these oblique impacts was selected for this study because the tests included here were part of a larger scope project aiming to compare the performance of the same restraint systems in frontal and oblique impacts. The current study focuses only on the results observed in the frontal sled tests. The reference belt system was a state-of-the-art, in-production, belt system including a retractor with a 2-kN pretensioner, a 4.5-kN force limiter, and a 3.5-kN outboard lap belt pretensioner (PT+FL). In the split buckle system, the belt webbing was separated at the buckle into one diagonal belt portion and one lap belt portion. The load limit at the retractor was increased to 6 kN and a pretensioner at
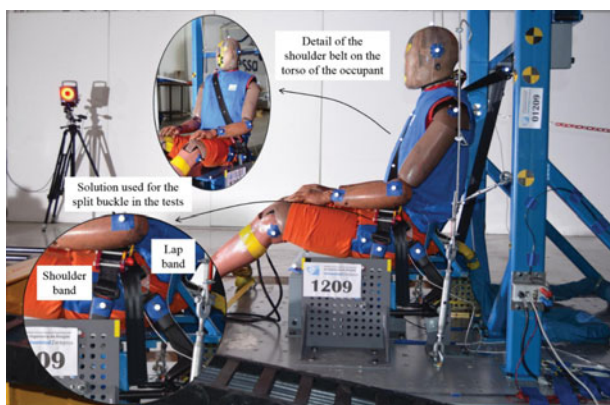

Figure 1. Test and simulation setup including split buckle.

either side of the lap belt was added. Sensor data were low-pass hardware filtered at 3 kHz and then filtered again using a CFC 600 low-pass filter (Society of Automotive Engineers 1998).

The THOR FE model and the Autoliv THUMS model were used for modeling. The Autoliv THUMS (Ver 1.4) model was derived from the THUMS model. The THUMS model was updated with a number of in-house modifications to improve its biofidelity (Pipkorn and Kent 2011; Pipkorn and Mroz 2008).

To evaluate the proposed belt concept, THOR and Autoliv THUMS simulations were carried out for both belt systems (PT+FL and SB; Table 1). For the reference system (PT+FL) the seat belt was mounted as in a vehicle on the passenger side. The position of the D-ring was kept constant when the SB seat belt was used. A preliminary parametric study with THUMS (Pipkorn et al. 2015) showed that optimal protection was achieved when the second buckle needed to connect the independent shoulder belt band was moved 150 mm forward of the conventional buckle position. The conventional buckle position was also similar to the one used with the PT+FL in an effort to test similar restraint conditions. Mechanical tests with both the reference and the split buckle systems were carried out with 3 repeats of each concept. Thereafter one PMHS test with the reference system and one test with the split buckle system was carried out. The complete test and simulation matrix is shown in Table 1. Sensor data were acquired at 10 kHz and filtered with a CFC 600 filter (Society of Automotive Engineers 1998). High-speed video images were recorded at 1 kHz. In the THOR tests 135 channels were recorded and shoulder and lab belt forces were measured by 4 load transducers attached to the belt (see Figure 1). PMHS tests were performed at the Impact Laboratory (I3A) of the University of Zaragoza and were carried out within the 7th Framework Program Marie Curie Action (Bio-Advance 2014). The initial occupant's position and belt geometry used in the sled tests are included in Table A2 (see online supplement). All procedures regarding the PMHS tests were reviewed and approved by the relevant ethics committee in the region (Ethics Committee for Clinical Research of Aragon).

Results

Main results (average ± SD) obtained in the sled tests and in the simulations with the different surrogates can be found in Table 2.

Seat belt forces

Peak diagonal belt force in the reference configuration for the PMHS was 4 kN and it occurred at 80 ms. For THUMS the predicted corresponding peak force was also 4 kN; however, the peak value occurred at 110 ms (Figure 2). In the mechanical
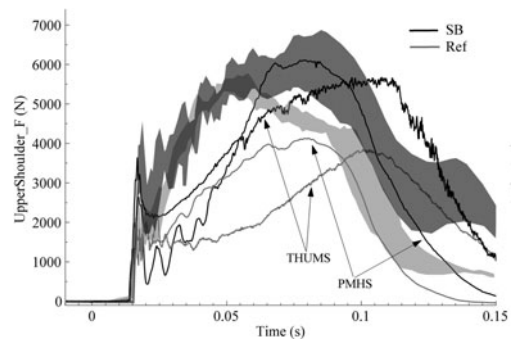
Table 1. Test and simulation matrix.

Occupant type	Restraint	Speed (km/h)
PMHS (1 run) mechanical test	SB	37.7
PMHS (1 run) mechanical test	PT+FL	34.6
THOR (3 runs) mechanical test	SB	34.8 + 0.2
THOR (3 runs) mechanical test	PT+FL	34.7 + 0.0
THUMS mathematical model	SB	35.0
THUMS mathematical model	PT+FL	35.0
THOR mathematical model	SB	35.0
THOR mathematical model	PT+FL	35.0

Figure 2. Diagonal belt force measured between the occupant's shoulder and the D-ring. Darker lines refer to the split buckle belt and lighter ones refer to the reference belt. Solid lines correspond to the PMHS tests and dashed lines are the corresponding THUMS predictions. Shaded areas are the force corridor measured with the THOR mechanical dummy (which includes the average ± 1 SD).

THOR tests the average peak force was 5.4 kN and it occurred at 53 ms. For the split buckle system, the peak force for the PMHS was 6 kN and it occurred at 80 ms; the corresponding predicted force with THUMS was 5.5 kN and it occurred at 110 ms. For THOR the average peak force was 6 kN and it occurred at 76 ms. THUMS prediction of the upper shoulder belt force peak value was accurate, although the predicted peak lagged the one measured in the PMHS tests. THOR predicted greater values than the ones measured in the PMHS tests and the peak magnitudes were reached earlier in the deceleration of the occupant.

Overall kinematics

Figures A6 and A7 (see online supplement) show selected still captures from the high-speed videos and simulations to illustrate the overall kinematics of the surrogates at different times during the impact.

Figure 3 shows the trajectories of the center of gravity of the head, the left acromion, and the lateral condyle of the proximal left tibia in the sagittal plane. Solid lines correspond to the PMHS trajectories and dotted lines are THUMS predictions to the trajectories. Black lines represent the SB system and grey lines represent the reference seat belt. PMHS and THUMS head excursion were greater for the split buckle configuration than for the system reference configuration (Figure 3). In the comparison between THUMS and PMHS, THUMS predicted greater head displacements than those observed in the PMHS tests. Regarding the displacement of the acromion the greatest PMHS shoulder excursion was for the split buckle configuration. For THUMS, shoulder excursion was similar for both the pretensioned load-limited and split buckle configurations.

Chest deflection and associated injury prediction

For the mechanical THOR dummy and THOR FE model the greatest chest deflections, in both resultant and x-direction, were measured in the reference configuration (Figure 4). Smaller chest deflections were observed for the split buckle system than for the reference belt system. For the mechanical THOR dummy,

Table 2. Peak value comparison of selected parameters between the PT+FL and the SB belt.

	Reference (PT+FL)				SB			
	THOR[a] mechanical	PMHS 1	THOR mathematical	THUMS	THOR[a] mechanical	PMHS 2	THOR mathematical	THUMS
Head acceleration[b] (g)								
x	−19.8 ± 2.8	10.4	−35.0	−6.8	−22.7 ± 1.4	28.5	−33.1	−6.5
y	3.9 ± 1.0	29.8	2.3	−0.8	2.3 ± 0.5	−58.1	6.7	−2.0
z	32.9 ± 2.0	33.5	35.0	7.5	38.4 ± 7.0	50.7	37.3	6.6
Head angle rate (°/s)								
	−767.1 ± 22.8	−2,170.0	−218	−245.8	−635.4 ± 99.5	2,078.1	−459.2	−32.7
y	−1,798.9 ± 92.0	579.8	−2,573	−1,114.0	−2,079.6 ± 149.8	419.8	−2,466.7	−1,068.0
z	−681.5 ± 18.1	300.4	−5,714	−0.4	−639.5 ± 110.7	1,001.0	−38.0	−0.4
Upper neck[c]								
F_x (kN)	1.2 ± 0.4	—	1.0		1.1 ± 0.0	—	1.0	
F_y (kN)	0.2 ± 0.0	—	−0.1		0.2 ± 0.1	—	−0.2	
F_z (kN)	1.4 ± 0.1	—	−2.0		1.8 ± 0.1	—	−1.8	
M_x (Nm)	−21.7 ± 3.1	—	−11.5		−19.0 ± 6.7	—	−15.8	
M_y (Nm)	22.0 ± 0.2	—	−23.2		21.6 ± 2.1	—	20.2	
M_z (Nm)	−5.4 ± 0.6	—	−5.3		2.9 ± 1.3	—	−5.3	
Lower neck								
F_x (kN)	0.6 ± 0.2	—	0.8		0.5 ± 0.1	—	0.8	
F_y (kN)	0.5 ± 0.3	—	−0.7		0.2 ± 0.1	—	−0.8	
F_z (kN)	−1.2 ± 0.2	—	−1.1		−1.6 ± 0.1	—	−1.6	
M_x (Nm)	23.8 ± 8.3	—	−42.7		25.5 ± 0.8	—	−65.3	
M_y (Nm)	55.0 ± 8.0	—	−149.7		58.8 ± 5.2	—	−107.4	
M_z (Nm)	−18.4 ± 4.1	—	−3.1		−19.1 ± 4.3	—	−4.3	
Pelvis acceleration (g)								
x	−11.3 ± 0.6	−38.7	−28.1	−44.3	−15.5 ± 0.9	−59.4	−28.5	−26.8
y	−9.3 ± 4.5	−36.4	−3.4	−19.5	−8.6 ± 4.1	27.7	−3.9	−40.8
z	−18.3 ± 1.7	−25.7	−28.9	−20.5	−19.0 ± 2.1	−22.6	−34.3	−14.5
Head maximum forward displacement (mm)	390.7 ± 11.1	188.8	345.4	376.0	406.4 ± 6.7	306.1	416.9	421.5
IR-TRACC (res, mm)								
Upper left	31.8 ± 1.5	—	33.2		32.1 ± 0.8	—	21.0	
Lower left	46.2 ± 3.4	—	30.8		32.4 ± 1.0	—	9.0	
Upper right	31.7 ± 2.9	—	19.7		31.8 ± 1.4	—	13.1	
Lower right	26.6 ± 2.9	—	10.1		21.4 ± 1.0	—	7.5	
IR-TRACC (x-direction, mm)								
Upper left	24.2 ± 0.5	—	32.5		25.1 ± 0.9	—	20.2	
Lower left	35.9 ± 5.6	—	25.8		24.5 ± 1.8	—	6.8	
Upper right	17.0 ± 14.3	—	18.9		8.0 ± 0.9	—	11.7	
Lower right	18.1 ± 8.0	—	6.7		12.3 ± 0.2	—	3.6	
Chest AIS 3+ injury risk (%)								
45-year-old	38				9			
65-year-old	77				24			
Number of rib fractures		5		0		2		0

[a] Values for THOR shown as average ± SD.
[b] Magnitude measured with respect to a local coordinate system with origin in the head attachment plate, not transferred to the head center of gravity.
[c] Including contribution from neck cables, although the tension in the cables was not measured in the tests.

peak chest deflection was obtained with the lower left IR-TRACC for all configurations except for the split buckle configuration in the x-direction, in which the maximum x-deflection was measured at the upper left location. For the THOR dummy model peak chest deflection was obtained with the upper left IR-TRACC for both configurations.

Based on the resultant deflection, the mechanical THOR tests using the reference system resulted in 38% risk of AIS 3+ thoracic injury for a 45-year-old occupant. Corresponding risk for a 65-year-old occupant was 77%. With the split buckle system the injury risk was reduced to 9% for a 45-year-old occupant and 24% for a 65-year-old occupant. The results from the THOR FE model resulted in 9% risk for a 45-year-old and 24% for a 65-year-old occupant with the reference system. For the split buckle system the risk was 1 and 2% for the 45- and 65-year-old, respectively.

The autopsy of the PMHS revealed that 5 rib fractures were observed in the test in which the reference seat belt was used, whereas only 2 rib fractures were found when the split buckle

seat belt was used. Interestingly, the majority of these fractures occurred at the left aspect of the ribcage in the case of the PT+FL seat belt, whereas the fractures were found on the right aspect for the SB system. Most fractures were monocortical without displacement for both seat belts. More details on the distribution of fractures are included in Figure A8 (see online supplement).

Discussion

Overall kinematics

Measurement of the displacement of the head in the sagittal plane in the mechanical tests with the THOR dummy resulted in small differences between the 2 belt systems. The peak forward displacement of the head center of gravity was similar regardless of the belt used (PT+FL: 390.7 ± 11.1 mm vs. SB: 406.4 ± 6.7 mm). However, the PMHS showed very different results in this case. For the PMHS there was an increase in head x-displacement with the split buckle system relative to the
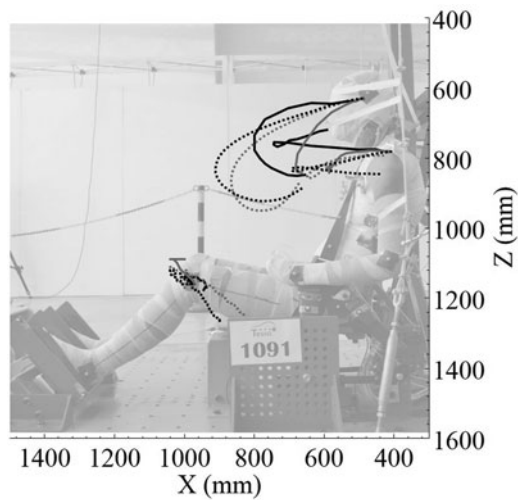
Figure 3. Head, shoulder and knee sagittal trajectories for PMHS and THUMS. Black lines correspond to the split buckle seat belt, and grey lines correspond to the reference seat belt. Solid lines are PMHS trajectories, and dashed lines are THUMS trajectories

excursion with the reference belt system (over 100 mm). One reason for the increase can be increased forward motion of the pelvis that resulted in reduced torso pitch. A contributing factor could be that the impact speed in the PMHS with the split buckle system was higher than in the other tests. As a future development, it would be interesting to check whether these differences can be observed in additional PMHS tests. In the PMHS test with the SB system, a trajectory in which the head moved forward first parallel to the local x axis and then underwent a curvilinear translation was observed. In the test with the PT+FL system there was almost no forward motion of the torso of the PMHS, resulting in a curvilinear translation of the head from the beginning of the deceleration. Consequently, the magnitude of the peak forward displacement of the head was smaller in this case (PT+FL: 188.8 mm vs. SB: 306.1 mm). However, analysis of the high-speed video images showed that whereas the SB lap belt prevented the forward displacement of the PMHS pelvis, the PT+FL belt allowed the pelvis of the occupant to move forward. Even if the displacement of the PMHS greater trochanter could not be tracked due to interference from the lap seat belt, the tibia markers can be used as proxy for the displacement of the pelvis. The peak forward displacement of the lateral condyle of the tibia was 69 mm with the PT+FL seat belt and only 29 mm when the
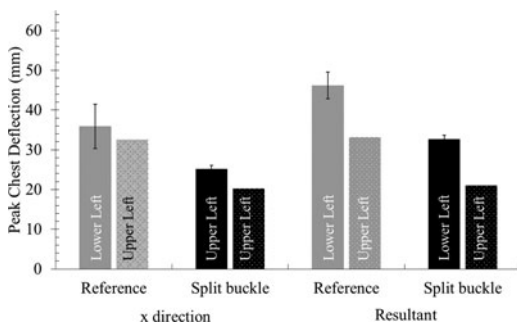

Figure 4. Peak chest deflection for mechanical THOR dummy and mathematical THOR dummy model. Solid bars are mechanical test results and dotted bars are mathematical model predictions. Error bars correspond to the standard deviation measured in the 3 repeats of mechanical THOR tests.

SB system was used (Figure 3). This difference can be attributed to the bilateral pretensioning of the lap belt. In addition, the high-speed video captures included in the Appendix (see online supplement) show that the feet of the PMHS using the PT+FL moved out of the foot restraint during the test ($t = 120$ ms). The flat design of the seat also plays a role in the deficient control of the motion of the pelvis as indicated in previous work using the same test fixture, although the seat was the same for both belt configurations.

These differences in the kinematics of the pelvis and the torso were not observed in the sled tests with the THOR dummy. Even if the pelvis of the dummy moves further forward, the torso of the dummy rotates up to the moment of maximum shoulder belt tension in which the head starts to undergo flexion. Several studies have stated that vertical motion of the H-point should be avoided and forward rotation of the upper body ideally beyond the vertical plane should be facilitated (Adomeit 1979; Adomeit and Heger 1975). In the tests, the pelvis motion was considered to fulfill the recommendations stated above. In none of the tests did the torso angle pass the vertical orientation. Regardless of the seat belt used, analysis of the kinematics of THOR does not indicate that submarining occurred in the tests.

Chest deflection and chest injuries

The decrease in THOR chest deflection confirmed one of the design goals of the split buckle system. Peak chest deflection was reduced by splitting the belt system and moving the lower attachment point of the diagonal belt forward in the vehicle while increasing the pretensioning force and adding a lap belt pretensioner. Moving the lower attachment point forward reduced the seat belt load in the lower part and increased the load in the upper part (clavicle) of the thorax. For the THOR, combining this with increased level of the force limiter, the excursion of the body was similar to that with the reference belt system and the chest deflection was reduced. In one of the FL+PT tests the right upper chest deflection in the x- and z-directions differed from corresponding measurements in the other 2 tests. However, the resulting right upper chest deflection was similar in all 3 tests. The reason for the difference in the measurements is not clear. However, one explanation can be that the THOR dummy is sensitive to the belt routing over the chest for deflection measurements in the x-, y-, and z-directions.

The reduced chest deflection for the THOR dummy was also reflected in the number of fractured ribs in the PMHS tests. The number of fractured ribs was lower for the split buckle system than for the reference belt system even though the impact speed and peak acceleration in the tests with the split buckle system was higher than in the test with the reference system. For the reference belt system there were 5 rib fractures (2L, 2R, 3R, 5R, 6R), whereas for the split buckle system there were two fractures (2R, 4R). The 2 PMHS included in the study were relatively young and very close in age. It is reasonable to assume that the benefits of the SB can be extrapolated to older subjects, in which the reduction of chest deflection and loading is essential to avoid life-threatening chest injuries (Kent et al. 2008). However, in the study results from 2 PMHS subjects were evaluated. Therefore,

to confirm the results from this study additional PMHS tests are needed.

The rib fracture predictions method proposed by Forman et al. (2012) was used to evelute the risk for an occupant to sustain 3+ rib fractures with the THUMS model. For the reference belt system THUMS predicted 0.65 and 0.91 risk for AIS 3+ fractures for a 45-year-old and a 65-year-old, respectively. For the split buckle belt system THUMS predicted 0.58 and 0.75 risk for AIS 3+ rib fractures for a 45-year-old and a 65-year-old, respectively. Peak first principal strain value for the reference belt system was 0.07 and for the split buckle system peak strain was 0.11. The number of rib fractures depends not only on belt force. Belt and chest geometry can influence rib fracture risk. In this study, there was one PMHS test run with each configuration. To improve and confirm the rib fracture predictions there is a need for more paired THUMS, THOR, and PMHS tests and simulations.

Other considerations

Recent studies have addressed different combinations of retractor pretensioning and force limiters to achieve an optimal chest deflection and kinematics (Forman et al. 2008, 2009; Kent et al. 2007).

Though other seat belt designs, such as those based on inflatable technologies, had shown a reduction in chest deflection at the cost of worsening other test results (Forman et al. 2010; López-Valdés et al. 2014), the results obtained with the SB seat belt are encouraging for exploring the benefits of complete independent control of the pelvis and torso during a crash.

The test buck was designed to approximate the seating position of a car occupant while allowing visual access for the cameras of the motion capture system. It is particularly suitable to ensure repeatability in a controlled loading environment that facilitates benchmarking human and dummy finite element models. It was originally conceived to isolate the kinematics of the torso from those of the pelvis and lower extremities by incorporating a knee bolster that was initially contacting the upper tibia of the occupants. In the tests carried out in this study, the knee bolster was eliminated to avoid restraining the lower limbs because oblique tests in exactly the same setup will be carried out in the future. Seat geometry and composition (i.e., foam and frame material properties) influence the kinematics of the vehicle occupant (Adomeit 1979); the effects of the seat were isolated from the effects of the belt restraint in the resulting kinematics. The test setup used in these experiments had been already utilized in a number of dummy, volunteer, and PMHS tests (Arbogast et al. 2009; Forman et al. 2013; López-Valdés et al. 2010; Seacrist et al. 2010; Shaw et al. 2009). Therefore, the test setup was considered a sufficiently valid representation of the boundary conditions of a restrained vehicle occupant.

In this study, a state-of-the-art belt system and belt geometry was used. Generally the compressive load in the spine with such a belt geometry is low. However, in future analyses with the SB system the loads on the spine will be evaluated.

Generally there was agreement between the kinematics of the THOR dummy model predictions and the mechanical THOR test results (Appendix A6, see online supplement). However, predicted head *z*-displacement was greater than the measured displacement. The chin of the mechanical THOR dummy was closer to the chest than the chin of the THOR dummy model was. In addition, rebound of the mathematical THOR dummy model was initiated earlier than for the mechanical THOR dummy. The predicted chest *x*-deflection and resulting deflection were consistently smaller than the measured chest deflections. However, reductions in chest deflections were shown in both the predictions and test results for the SB system relative to the reference belt system.

Limitations

To evaluate the physical test setup, the physical tests using THOR similar to the Mod-Kit SD3 shoulder were compared to the virtual test setup using the THOR FE model, which was a beta version of the THOR-M. Even if the test fixture was utilized before in the assessment of the biofidelity of ATDs and in the development of thoracic ATD injury criteria, its utility in the assessment of restraint systems is questionable. The simple geometry and the completely rigid structure of the seat facilitated the forward motion of the pelvis of the PMHS restrained with the PT+FL and the subsequent differences in torso pitch with respect to the other seat belt solution. A regular production seat would have reduced the forward motion of the pelvis and contributed to increase the forward rotation of the torso.

One additional limitation is the magnitude variability observed in the deceleration pulse in the 2 PMHS experiments that reached almost 4 *g* at its peak difference. Although this difference would have hindered a detailed quantitative comparison between the performance of the 2 systems, the differences in the nature of the kinematics suggest that these differences were not related just to a change in the magnitude of the mechanical insult but to the way in which the restraints interacted with the PMHS. Interestingly, these differences were not observed when the surrogate chosen was THOR.

Some channels of the external data acquisition system malfunctioned during the THOR tests. In particular, the upper shoulder belt load cell was not measuring the tension of the belt correct. To overcome this issue, a methodology was developed so that the magnitude of the belt tension at the upper shoulder location could be estimated using the measurement from the lower shoulder belt. The correlation factors of the relationship found between the upper and lower belt tension magnitudes were $R^2 = 0.98$ (PT+FL) and $R^2 = 0.99$ (SB). More details on the shoulder belt force estimation are included in Figures A4 and A5 (see online supplement).

impact biomechanics, signed on Feb 11th, 2015. The PMHS tests were performed within the Bio-Advance project (Marie Curie Actions, FP7/2007–2013, REA grant agreement no. 299298). More information about this project can be found in the final report included in the references. The analyses presented here were not generated during the project and do not represent necessarily the position of the researchers involved in Bio-Advance. This study is solely the interpretation of the authors and is not necessarily the view of Instituto Aragones de Fomento.

References

Adomeit D. Seat design—a significant factor for safety belt effectiveness. In: *Proceedings of the 23rd STAPP Car Crash Conference*. San Diego, CA; 1979:41–68.

Adomeit D, Heger A. Motion sequence criteria and design proposals for restraint devices in order to avoid unfavorable biomechanic conditions and submarining. Paper presented at: 19th Stapp Car Crash Conference; 1975; Warrendale, PA.

Arbogast K, Balasubramanian S, Seacrist T, Maltese M, García-España F. Comparison of kinematic responses of the head and spine for children and adults in low-speed frontal sled tests. In: *Proceedings of the 53rd Stapp Car Crash Conference*; Savannah, GA; 2009: 329–372.

Bio-Advance. *Advancing Traffic Safety through the Investigation of Human Tolerance to Impact. Marie Curie Actions*. Final Report. Zaragoza: European Commission; Project No. 299298 2014.

Cummings P, Wells JD, Rivara FP. Estimating seat belt effectiveness using matched pair cohort methods. *Accid Anal Prev.* 2003;35: 143–149.

Department of Transportation. *New Car Assessment Program (NCAP), Request for Comments.* Washington, DC: Author; 2015. Docket No. NHTSA-2015-0119.

Forman JL, Kent R, Morz K, Pipkorn B, Boström O, Segui-Gomez M. Predicting rib fracture risk with whole-body finite element models: development and preliminary evaluation of a probabilistic analytical framework. *Annu Proc Assoc Adv Automot Med.* 2012:56:109–124.

Forman J, López-Valdés F, Lessley D, Kindig M, Kent R, Ridella S, Boström O. Rear seat occupant safety: an investigation of a progressive force-limiting, pretensioning 3-point belt system using adult PMHS in frontal sled tests. In: *Proceedings of the 53rd Stapp Car Crash Conference*; 2009;53:49

Forman JL, López-Valdés FJ, Dennis N, Kent R, Tanji H, Higuchi K. An inflatable belt system in the rear seat occupant environment: investigating feasibility and benefit in frontal impact sled tests with a 50th percentile male ATD. *Annu Proc Assoc Adv Automot Med.* 2010;54:111–126.

Forman JL, López-Valdés F, Lessley D, et al.. Occupant kinematics and shoulder belt retention in far-side lateral and oblique collisions: a parametric study. Paper presented at: 57th Stapp Car Crash Conference; 2013.

Forman J, Michaelson J, Kent R, Kuppa A, Bostrom O. Occupant restraint in the rear seat: ATD responses to standard and pre-tensioning, force-limiting belt restraints. *Annu Proc Assoc Adv Automot Med.* 2008;52:141–154.

Gabler HC, Fitzharris M, Scully J, Fildes BN, Digges K, Sparke L. Far side impact injury risk for belted occupants in Australia and the United States. Paper presented at: International Technical Conference on the Enhanced Safety of Vehicles; 2005.

Humanetics. *THOR-50TH Dummy Model LS-DYNA.* Release Ver 0.6. Plymouth, MI: Author; 2014.

Kent R, Crandall J, Bolton J, Prasad P, Nusholtz G, Mertz H. The influence of superficial soft tissues and restraint conditions on thoracic skeletal

injury prediction. In: *Proceedings of the 45th Stapp Car Crash Conference*; San Antonio, TX; 2001:183–204.

Kent R, Forman J, Parent D, Kuppa S. Rear seat occupant protection in frontal crashes and its feasibility. *Paper presented at: International Technical Conference on the Enhanced Safety of Vehicles (ESV)*; 2007.

Kent R, Henary B, Matsuoka F. On the fatal crash experience of older drivers. *Annu Proc Assoc Adv Automot Med.* 2005;49:371–391.

Kent R, Woods W, Bostrom O. Fatality risk and the presence of rib fractures. *Annu Proc Assoc Adv Automot Med.* 2008;53:73–84.

López-Valdés F, Juste-Lorente O. Innovative restraints to prevent chest injuries in frontal impacts. Paper presented at: 24th Technical Conference on the Enhanced Safety of Vehicles; 2015; Gothenburg, Sweden.

López-Valdés F, Juste Lorente O, Pipkorn B, et al. A comparison of the performance of two advanced restraint systems in frontal impacts. *Traffic Injury Prev.* 2014;15(Suppl 1):S119–S125.

López-Valdés F, Lau JJ, Lamp J, et al. Analysis of spinal motion and loads during frontal impacts, comparison between PMHS and ATD. *Annu Proc Assoc Adv Automot Med.* 2010;1404(1398):1402.

Parent D, Craig M, Ridella S, McFadden J. Thoracic biofidelity assessment of the THOR Mod Kit ATD. Paper presented at: 23rd Technical Conference on Enhanced Safety of Vehicles; 2013.

Pipkorn B, Kent R. Validation of a human body thorax model and its use for force, energy and strain analysis in various loading conditions. Paper presented at: International Research Council on Biomechanics of Injury (IRCOBI); 2011.

Pipkorn B, López-Valdés F, Juste-Lorente O, Maza M, Sunnevång C. Study of the kinematics of the THOR dummy in nearside oblique impacts. Paper presented at: International Research Council on Biomechanics of Injury (IRCOBI); 2016.

Pipkorn B, López-Valdés F, Lundgren C, Bråse D, Sunnevång C. Innovative seat belt system for reduced chest deflection. Paper presented at: 24th Technical Conference on Enhanced Safety of Vehicles; 2015; Gothenburg, Sweden.

Pipkorn B, Mroz K. Validation of a human body model for frontal crash and its use for chest injury prediction. Paper presented at: SAE Digital Human Modeling for Design and Engineering Conference; 2008; Pittsburgh, PA.

Roser M. Life expectancy. 2016. Available at: http://ourworldindata.org/data/population-growth-vital-statistics/life-expectancy/.

Rouhana SW, Bedewi PG, Kankanala SV, et al.. Biomechanics of 4-point seat belt systems in frontal impacts. Paper presented at: 47th Stapp Car Crash Conference; 2003.

Saunders J, Parent D, Ames E. NHTSA oblique crash test results: vehicle performance and occupant injury risk assessment in vehicles with small overlap countermeasures. Paper presented at: 24st ESV Conference; 2015; Gothenburg, Sweden.

Scarboro M. Real world older occupant injury. Paper presented at: SAE Government/Industry Meeting; January 2014; Washington, DC.

Seacrist T, Balasubramanian S, García-España F, et al.. Kinematic comparison of pediatric human volunteers and the Hybrid III 6-year-old anthropomorphic test device. *Annu Proc Assoc Adv Automot Med.* 2010;54:97–108.

Shaw G, Parent D, Purtsezov S. Impact response of restrained PMHS in frontal sled tests: skeletal deformation patterns under seat belt loading. In: *Proceedings of the 53rd Stapp Car Crash Conference*; Savannah, GA; 2009:1–48.

Society of Automotive Engineers. *Instrumentation for Impact Test.* Warrendale, PA: Author; 1998. Document No. J211.

Sunnevång C, Hynd D, Carroll J, Dahlgren M. In: *Proceedings of the International Research Council on Biomechanics of Impact (IRCOBI)*; Berlin, Germany; 2014:377–388.

Walz M. NCAP test improvements with pretensioners and load limiters. *Traffic Inj Prev.* 2004;5:18–25.